Tikrit Journal of Engineering Sciences (2025); 32(3): 1968
DOI: http://doi.org/10.25130/tjes.32.3.36

IRAQI Academic Scientific Journals

ISSN: 1813-162X (Print); 2312-7589 (Online)

Tikrit Journal of Engineering Sciences

available online at: http://www.tj-es.com

TJES Tikrit Journal of Engineering Sciences

Development of Two-Step Model Predictive Control for an Adaptive Cruise Control System

Farah M. Ali *, Nizar H. Abbas

Department of Electrical Engineering, Engineering College, University of Baghdad, Baghdad, Iraq.

Keywords:

Adaptive Cruise Control; Collision Avoidance; Mathematical Program; Model Predictive Control; Vehicle Dynamics.

Highlights:

- *ACC adapts its speed automatically to follow the vehicle ahead based on the changes in traffic conditions.*
- *Model predictive control manages different driving scenarios in real-time.*
- *The simulation was performed using MATLAB.*

ARTICLE INFO

Article history:

Received	12 Jan.	2024
Received in revised form	23 Jan.	2024
Accepted	01 Oct.	2024
Final Proofreading	21 Aug.	2025
Available online	28 Aug.	2025

© THIS IS AN OPEN ACCESS ARTICLE UNDER THE CC BY LICENSE. http://creativecommons.org/licenses/by/4.0/

Citation: Ali FM, Abbas NH. **Development of Two-Step Model Predictive Control for an Adaptive Cruise Control System**. *Tikrit Journal of Engineering Sciences* 2025; **32**(3): 1968.
http://doi.org/10.25130/tjes.32.3.36

***Corresponding author:**

Farah M. Ali

Department of Electrical Engineering, Engineering College, University of Baghdad, Baghdad, Iraq.

Abstract: This paper introduces an adaptive cruise control (ACC) of a vehicle based on Model Predictive Control (MPC) as a high-level controller of the ACC system. This high-level controller calculates the desired acceleration for a low-level controller. Also, this paper presents a longitudinal dynamic model of a vehicle consisting of the dynamics of the powertrain and the dynamics of external forces. In addition to establishing a steady spacing distance between two vehicles, avoiding collision, and keeping the acceleration calculation within permitted limits, a method is proposed to speed up the algorithm and reduce the computational effort. Finally, two driving scenarios were used to validate the proposed method, and a comparison of the performance between the original MPC and the speedup MPC was introduced. The simulation results showed that the host vehicle tracked the preceding vehicle accurately for the proposed controller without collision. Moreover, it showed that the execution time required for the proposed method was less than that of the original MPC controller.

تطوير نموذج التحكم التنبؤي ذو الخطوتين لنظام التحكم التكيفي في السرعة

فرح مهدي علي، نزار هادي عباس
قسم الهندسة الكهربائية/ كلية الهندسة / جامعة بغداد / بغداد – العراق.

الخلاصة

تقدم هذه الورقة نظام تثبيت السرعة التكيفي (ACC) للمركبة استنادًا إلى التحكم التنبؤي للنموذج (MPC) كوحدة تحكم عالية المستوى لنظام ACC. تقوم وحدة التحكم عالية المستوى هذه بحساب التسارع المطلوب لوحدة التحكم ذات المستوى المنخفض. كما يقدم هذا البحث نموذجا ديناميكيا طوليا للمركبة يتكون من ديناميكية مجموعة نقل الحركة وديناميكية القوى الخارجية. بالإضافة إلى إنشاء مسافة تباعد ثابتة بين مركبتين، وتجنب الاصطدام، والحفاظ على حساب التسارع ضمن الحدود المسموح بها، تم اقتراح طريقة لتسريع الخوارزمية وتقليل الجهد الحسابي. وأخيرا، يتم استخدام سيناريوهين للقيادة للتحقق من صحة الطريقة المقترحة، ويتم تقديم مقارنة الأداء بين MPC الأصلي وMPC المسرع. أظهرت نتائج المحاكاة أن المركبة المضيفة تتبع المركبة المتقدمة بدقة لوحدة التحكم المقترحة دون اصطدام. علاوة على ذلك، يوضح أن وقت التنفيذ المطلوب للطريقة المقترحة أقل من زمن تنفيذ وحدة التحكم MPC الأصلية.

الكلمات الدالة: نظام تثبيت السرعة التكيفي، تجنب الاصطدام، البرنامج الرياضي، التحكم التنبؤي بالنموذج، ديناميكيات السيارة.

1.INTRODUCTION

In recent years, the number of automobiles on the road has grown faster than the number of road resources, which has led to significant issues with traffic congestion and accidents [1, 2]. Consequently, it is essential to enhance driving controls to lower the number of accidents and ensure safety measures. Adaptive Cruise Control (ACC) is considered one of the Advanced Driver Assistance Systems (ADAS) that adapts its speed automatically to follow the vehicle ahead according to changes in traffic conditions. ACC systems were developed to improve the functionality of conventional CC systems. Thus, ACC effectively removes one of the key risk factors that contribute to rear-end crashes [3]. In addition to preventing congestion and traffic accidents, ACC can reduce drivers' workloads and increase economic efficiency. Adaptive cruise control systems utilize various sensors to enhance driving safety and comfort. These sensors include radar sensors, speed sensors, front detection sensors, lane detection sensors, and camera sensors. Mohammed et al. [4] revealed that camera-based systems offered shorter following distances relative to ISO standards (increasing traffic capacity but raising safety concerns), while radar-based and combined camera and radar-based systems provided larger following distances, i.e., enhanced traffic safety but diminished capacity. Considerable research on the ACC system has been done. Vibhor et al. [5] used model predictive control to evaluate the host vehicle's spacing-control laws for transitional maneuvers (TM). The performance of the transitional maneuver was formulated and solved as an optimal control problem (OCP). Payman et al. [6] introduced two control application designs for ACC: the gain-scheduling Linear Quadratic (GSLQ) and gain-scheduling proportional integral (GSPI) control. Zhu et al. [7] designed a two-layer controller; the upper layer calculates the expected acceleration of the vehicle through an optimal control method, while the lower layer utilizes the μ control method to improve the robustness of the suggested controller. Model predictive control (MPC) is presented as an approach to solving the multiple input/ multiple output problem [8, 9]. MPC is one method that utilizes explicit models to predict the system's future behaviour [10]. It is one of the most effective methods to manage different driving scenarios in real-time conditions while preserving a logical optimization-based control. Introducing the MPC algorithm into the ACC system has generated high academic interest. Pratama et al. [11] used neural network predictive control (NNPC) to develop a new approach to controller design to simulate vehicle features and MPC to reduce the quadratic error between future reference paths and estimated values. Yanzhao et al. [12] formulated an optimized speed trajectory for the ACC system of an electric vehicle (EV) to lower fuel usage by establishing an MPC-based energy-optimal ACC function. Moreover, to handle measurement uncertainty and disturbances, Shilin et al. [13] applied an extended state Kalman filter to determine the state and disturbance magnitude. They utilized an explicit MPC (EMPC) where a binary search tree was utilized to decrease the computation load. Zengfu et al. [14] also addressed the disturbances by suggesting a novel MPC-based adaptive cruise control algorithm and active disturbance rejection control (ADRC) to increase control precision and restrain the disturbance. Zhan et al. [15] proposed a robust optimal ACC strategy to achieve tracking performance and driving comfort of adaptive cruise control for intelligent vehicles under bounded matching disturbances. First, an optimal controller is designed to realize driving safety and comfort. Then, the unknown parameter is approximated by Adaptive Dynamic Programming to solve the optimal control law, and Lyapunov analysis is used for the asymptotic stability and Uniformly Ultimately Bounded stability. Iman et al. [16] used experimental data based on real-world conditions to investigate the effect of automated and cooperative systems in traffic, including traditional, ACC, and CACC vehicles. Payman et al. [17] proposed a Nonlinear Model Predictive Control (NMPC) algorithm in

designing ACC and CC systems. Depending on the current traffic situation, switching between ACC and CC is performed automatically to predict future reference paths according to a specified distance and speed. Lie et al. [18] proposed an ACC algorithm based on MPC with a higher-order kinematics model that examines the changing characteristics of model parameters. Zifei et al. [19] satisfied multi-objectives, such as eco-driving, safety issues, comfort riding, and tracking capability, by designing the ACC system using the model predictive control algorithm. The results of the proposed system were compared with those of the conventional PID controller. Antonio et al. [20] developed an adaptive MPC for controlling the Cooperative ACC scenario of two vehicles. During a cut-in maneuver, a safety evaluation was performed as the number of platooning vehicles was extended to four. Oscar et al. [21] proposed an adjusted shifting strategy for the Real-Time Iteration (RTI) method, which maintained recursive feasibility and stability characteristics. This method reduces the computational burden associated with the MPC significantly. Two modes of longitudinal control are used in the ACC system. The first mode is the speed control mode (cruise control CC), which becomes active if no vehicle is encountered in front of the ACC vehicle (host vehicle). The second mode is the distance control mode (following mode), which becomes active when a preceding vehicle is ahead. The ACC vehicle faces two situations: the steady-state operations (a constant speed preceding vehicle ahead) and the transient operations. The latter situation may occur when the ACC vehicle encounters a slower or halted vehicle ahead, during a cut-in, or a sudden stop by a preceding vehicle or stop-and-go situation. The host vehicle must have a high-accuracy tracking capability in all the mentioned situations. The contribution of this study is to lower the computational burden for the MPC and speed up the algorithm execution using a two-step prediction of the control law, which simulates a parallel calculation of the input control. The rest of this paper is organized as follows: Section 2 describes the mathematical modeling problem, Section 3 explains the control methodology using an MPC controller, and Section 4 describes the proposed MPC for ACC as optimal control. The simulation results are shown in Section 5. Finally, Section 6 shows the conclusion of the paper.

2.VEHICLE MODEL

The vehicle's dynamic is categorized into:

1) The powertrain dynamic includes the engine, torque converter, gearbox, and final drive.
2) The dynamic considering the external forces.

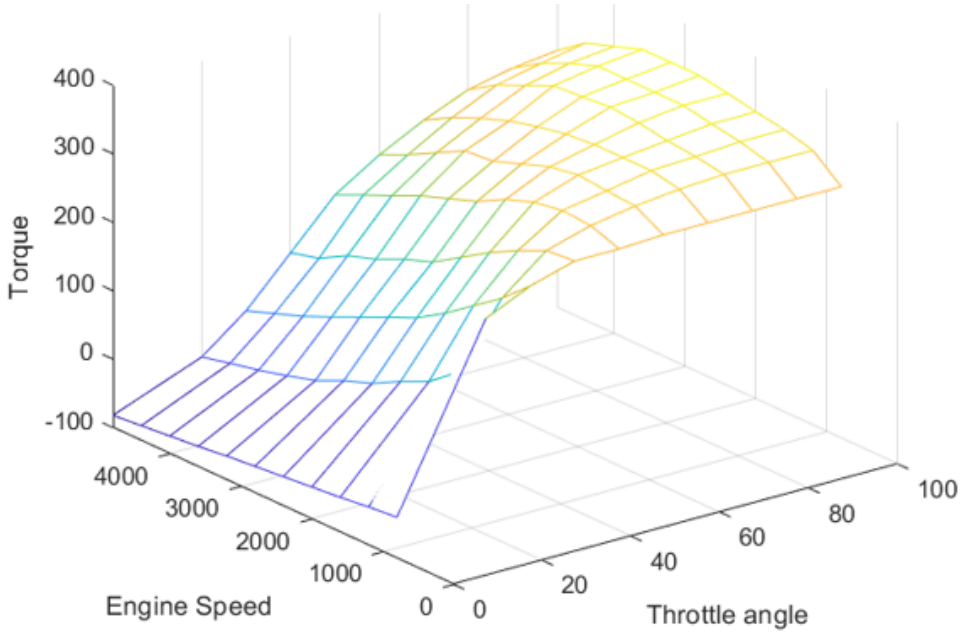

Fig. 1 Torque as a Function of Throttle and Different Engine Speeds.

2.1.Powertrain Dynamic

2.1.1.Engine Model Using Maps

The first-order model of the engine consists of a single state variable (ω_e). The equation of (ω_e) is expressed by [22, 23]:

$$I_e\dot{\omega}_e = T_{net}(\alpha, \omega_e) - T_{load} \quad (1)$$

where I_e is engine inertia, T_{load} is the load torque, and T_{net} (function of the engine speed ω_e and throttle angle α) is the net torque with losses; also, it is considered a steady state. T_{net} can be obtained from the map shown in Fig. 1 (MATLAB Simulink map).

2.1.2.Torque Convertor Model

The torque converter characteristics are usually described using the following parameters (as shown in Fig. 2) [24]:

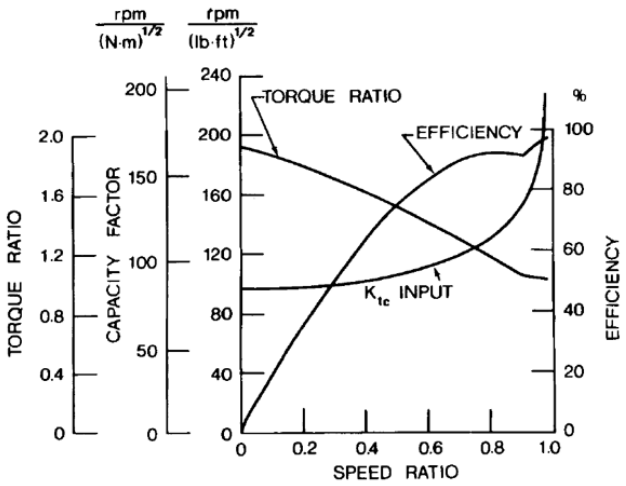

Fig. 2 Torque Converter Characteristics.

Speed ratio (C_{sr})= output speed/input speed:

$$C_{sr} = \omega_t/\omega_i \quad (2)$$

Torque ratio (C_{tr})= output torque/input torque:

$$C_{tr} = T_t/T_i \quad (3)$$

$$\eta_c = C_{sr}C_{tr} \quad (4)$$

$$K_{tc} = \frac{speed}{\sqrt{torque}}$$

(K_{tc}) provides information about the converter's ability to transmit or absorb torque. It is proportional to the square of the engine's speed (see Fig. 3) [24].

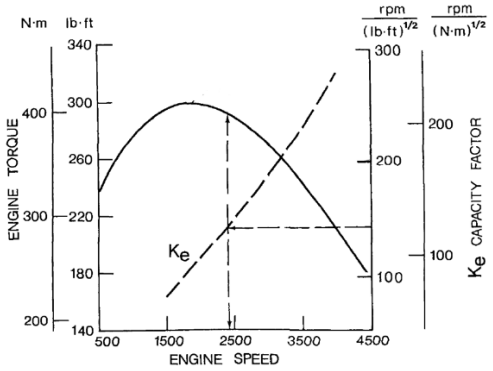

Fig. 3 Curve of Capacity Factor of an ICE Engine.

Table 1 Powertrain Dynamic Parameters.

Parameter	Description
C_{sr}	speed ratio
C_{tr}	torque ratio
ω_t	output speed
ω_i	input speed
T_t	the output torque of the converter
T_i	input torque of the converter
η_c	Efficiency factor
K_{tc}	capacity factor
ω_e	rotation speed of the engine
T_{out}	transmission output torque
T_{in}	transmission input torque
R_{tr}	transmission ratio
ω_{out}	transmission output speed
ω_{in}	transmission input speed

The input torque of the converter can be described as:

$$T_i = (\frac{\omega_e}{K_{tc}})^2 \quad (5)$$

The capacity factor range of the engine and converter must be identical to match correctly, so that:

$$K_e = K_{tc}$$

By rewriting Eqs. (2) and (3), the torque converter equation becomes:

$$T_t = C_{tr} \times T_i,$$

$$\omega_t = C_{sr} \times \omega_i,$$

The torque converter outputs (speed and torque) should equal the gearbox's input characteristics. Thus, the outputs of the gearbox are:

$$T_{out} = R_{tr} \times T_{in} \quad (6)$$

$$\omega_{out} = \omega_{in}/R_{tr} \quad (7)$$

The (R_{tr}) differs according to the gear set value.

2.2.Vehicle's Dynamics with External Forces

2.2.1.Longitudinal Tire Force

In this paper, no lateral movement of the vehicle is investigated. It is essential to define an axis system for parameters to describe the characteristics of a tire's moment and the acting forces. Figure 4 [24] shows a standard axis system suggested by the "Society of Automotive Engineers."

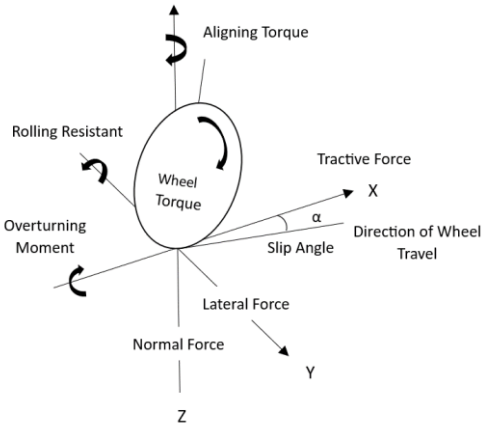

Fig. 4 The Tire Axis.

A force balance along the vehicle's longitudinal axis yields:

$$m\ddot{x} = F_{xf} + F_{xr} - F_{aero} - R_{xf} - R_{xr} \pm F_g \quad (8)$$

Table 2 Vehicle's Dynamic Parameters.

Parameter	Description
m	mass of the vehicle
$\ddot{x}$	acceleration of the vehicle
F_{xf}	front longitudinal tire force
F_{xr}	rear longitudinal tire force
F_{aero}	longitudinal aerodynamic drag force
R_{xf}	rolling resistance force at the front tires
R_{xr}	rolling resistance force at the rear tires
F_z	normal force exerted on the tire
J_w	moment of inertia of the wheels
$\dot{\omega}$	angular acceleration of the wheel
T_w	wheel torque
T_b	brake torque
R_w	wheel radius
g	Gravitational acceleration
θ	road's angle of inclination
C_r	rolling resistance coefficient
ρ	the mass density of the air
C_d	coefficient of aerodynamic resistance
A	frontal area of the vehicle
V	vehicle's speed

These forces are presented in Fig. 5.

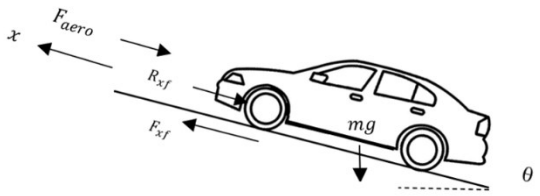

Fig. 5 Vehicle's Dynamic with Acting Forces.

a) Traction force (F_x)

The amount of traction parallel to the axis of motion is known as the traction force. Pacejka [25] designed the "Magic Formula," a series of tire models. These models suit a broad range of tire types and operating conditions. Based on the percentage of longitudinal slip, the Pacejka formula determines the longitudinal force of the tire. The Magic Formula given by Pacejka is:

$$\mu(\sigma) = D.sin\{C.arctan(B.\sigma - E.(B.\sigma - arctan(B.\sigma)))\} \quad (9)$$

where $\mu(\sigma)$ is the friction coefficient, σ is the slip ratio, and B, C, D, and E are fitting constants, i.e., describe various road conditions, as tabulated in Table 3.

Table 3 Pacejka Formula Coefficients for Different Surface Types.

Road type	B	C	D	E
Dry Tarmac	10	1.9	1	0.97
Wet Tarmac	12	2.3	0.82	1
Snow	5	2	0.3	1
Ice	4	2	0.1	1

The longitudinal traction force F_x can be calculated from:

$$F_x = \mu(\sigma)F_z \quad (10)$$

Figure 6 shows an example of slip ratio change for specific road conditions.

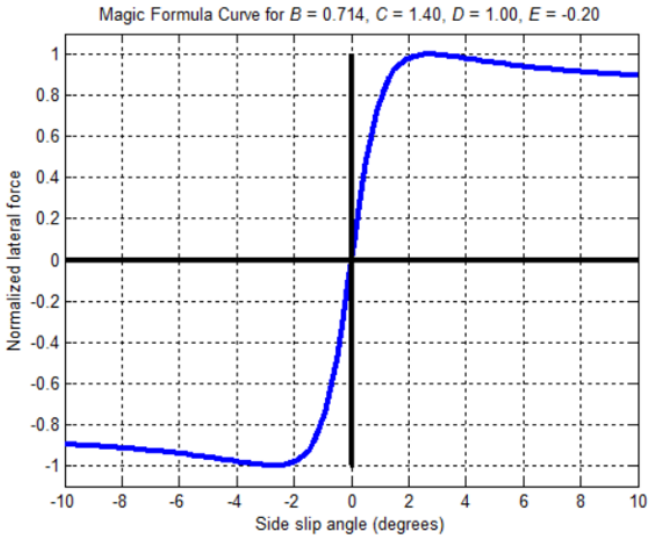

Fig. 6 Normalized Tire Force vs. Slip Ratio Angle.

b) Gravitational force (F_g):

When traveling upwards or downwards, the vehicle is significantly impacted by gravity. The force of gravity pulls the car in the opposite direction (negative sign), while it travels upward, slowing it down. In contrast, driving downward forces the vehicle to accelerate (positive sign).

$$F_g = \pm mgsin(\theta) \quad (11)$$

c) Rolling resistance (R_x):

The force resisting a body moving on a surface is known as rolling resistance. The generic equation is expressed as:

$$R_x = mgC_r\cos(\theta) \quad (12)$$

The rolling resistance coefficient is affected by factors like wheel design, rolling surface, wheel dimensions, and more [24].

2.2.2.Aerodynamic Force

Two sources generate the aerodynamic resistance: The airflow across the vehicle body and the flow through the radiator system, i.e., with the first forming more than 90% of the total resistance force [24]. In practice, the aerodynamic resistance is a function of the vehicle's speed. It is stated as follows:

$$F_{aero} = \frac{\rho}{2} AC_dV^2 \quad (13)$$

- **Wheel dynamic:**

The wheel dynamic for the front and rear axles is stated below [23]:

$$J_w\dot{\omega} = T_w - T_b - R_w F_x \quad (14)$$

3.CONTROLLER *DESIGN*

Two-level controllers can be decoupled to simplify the design and allow faster control rates. The high-level controller (HLC) represents a planner that calculates the desired acceleration ($\ddot{x}_{des}$) of the ACC vehicle and the low-level controller (LLC), assuring the selection of appropriate throttle and brake values (u_t, u_b), as shown in Fig. 7.

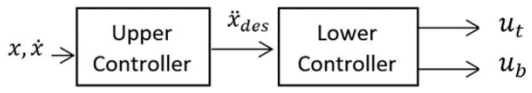

Fig. 7 Two-Level Controller Structure.

In this architecture, a dedicated planning (HLC) part could be performed offline and does not require running as fast as the inner loop (LLC). The reference or desired acceleration ($\ddot{x}_{des}$) is obtained from the velocity of the host vehicle ($\dot{x}$), the distance from the preceding vehicle (x), the desired driver's speed (v_{des}), and the desired distance (d_{des}). The desired distance headway, d_{des}, can be computed using the Constant-Time Headway policy as:

$$d_{des} = v.t_h + d_{safe} \quad (15)$$

where v is the following vehicle velocity, and (t_h) is the constant-time headway, defined as the time the ACC vehicle takes to reach the point where the leading vehicle is at its present speed. (d_{safe}) is the additional distance between two vehicles to avoid a collision.

3.1.MPC Controller

The main working principle of the MPC can be summarized as having a system in which its action is forecasted depending on the model. Another principle in MPC is to use measurements of the past to determine the most likely initial state of the system. These records are reconciled with the model measurements to obtain the most likely value of the state at the current time. The error between actual and predicted values can be optimized (minimized) using feedback. In addition, the forecasted model's fault is refined according to the reference output. The optimal control sequence can be determined by solving an online optimization problem. Only the initial value of this sequence is used to control the system. Then, the control horizon moves one step ahead, and the MPC control process is repeated. Therefore, the fundamental characteristics of this control technique, such as prediction, receding horizon, and feedback mechanism, fulfill the requirements for an excellent and robust controller. At the HLL, the MPC controller determines the desired acceleration ($\ddot{x}$) for the ongoing traffic condition. Then, the LLC decides to apply the throttle (u_t) or brake (u_b). The basic block diagram of the controller is shown in Fig. 8.

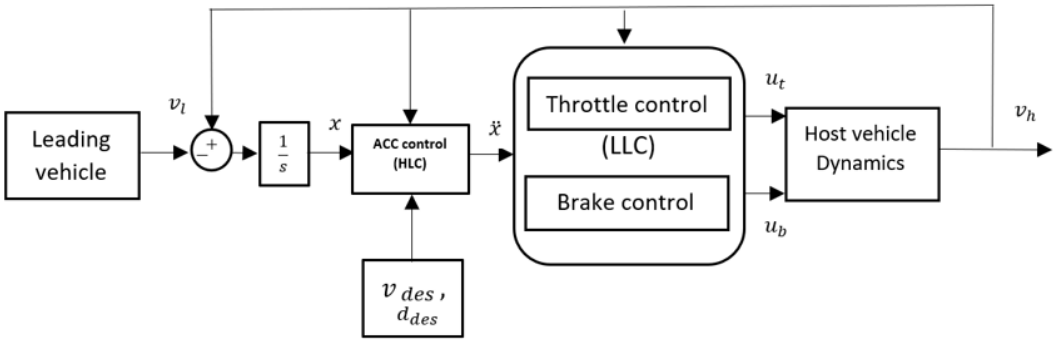

Fig. 8 The Block Diagram of the ACC System.

The kinematic relationship representing the host vehicle and the leading vehicle is modeled, as shown in Fig. 9:

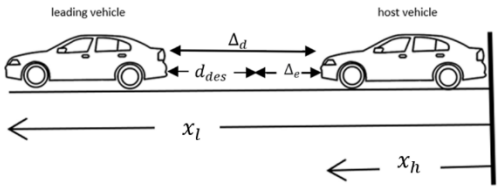

Fig. 9 The Host and Leading Vehicles Model.

The relative distance Δ_d is:

$$\Delta_d = x_l - veh_{length} - x_h \quad (16)$$

where veh_{length} represents the leading vehicle length.

In the ACC system, a control algorithm must be applied to maneuver the vehicle to a specified inter-vehicle distance (SIVD) called a transitional maneuver. Also, this distance must be maintained by the ACC vehicle (steady-state operation) [5]. Since ACC aims to maintain a desired gap between the host and target vehicle d_{des}, a certain consideration for the MPC algorithm is taken below:

1- The distance error, (Δ_e), is defined as the difference between the gap distance Δ_d (also called range) and the desired distance, d_{des}, where

$$\Delta_e = \Delta_d - \boldsymbol{d_{des}} \quad \textbf{(17)}$$

(Δ_e should converge to zero.)

2- The velocity difference, Δ_v (also called range rate), is defined as the difference between the preceding vehicle velocity, v_l, and host velocity, v_h, where:

$$\Delta_v = \boldsymbol{v_l - v_h} \quad \textbf{(18)}$$

(Δ_v should converge to zero, too.)

Track smoothly desired acceleration ($\ddot{x}$).

3- Reach and maintain a safe inter-vehicle distance (d_{des}) and act quickly in dangerous situations (avoiding collision with the leading vehicle during TM).

The range Δ_d and velocity difference Δ_v between the two vehicles are used by the HLC to determine the desired acceleration commands. See Fig. 10 [26].

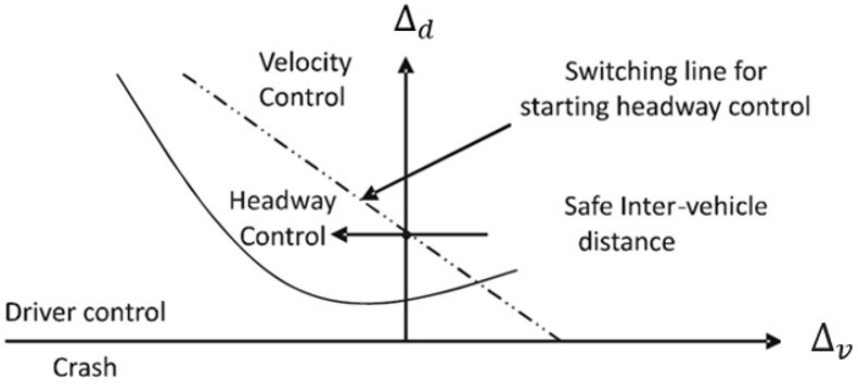

Fig. 10 Range vs. Range Rate Diagram.

The continuous-time state space of the system can be written as:

$$\begin{aligned} \dot{\boldsymbol{x}} &= \boldsymbol{A\,X + B\,u} \\ \boldsymbol{y} &= \boldsymbol{C\,X + D\,u} \end{aligned} \quad \textbf{(19)}$$

The state variable of the plant can be defined as:

$$X = [x_1 \quad x_2 \quad x_3]^T$$

with $x_1 = x_h$(host car absolute position), $x_2 = \dot{x}_h$(host car velocity), and $x_3 = \ddot{x}_h$(host car acceleration). In the literature, the MPC-controlled system is generally modeled by a discrete-time state space model. Hence, a discretized model is obtained as below [26]:

$$\begin{aligned} \boldsymbol{X(k+1)} &= \mathbf{A}\,\boldsymbol{X(k)} + \mathbf{B}\,\boldsymbol{u(k)} \\ \boldsymbol{y(k)} &= \mathbf{C}\,\boldsymbol{X(k)} + \mathbf{D}\,\boldsymbol{u(k)} \end{aligned} \quad \textbf{(20)}$$

where k is the kth sampling point, u is the control input, **A**, **B**, **C**, and **D** are the state-space matrices, and y is the system output. The matrix **D** is assumed to be zero (the control input u does not influence the output y) [27].

The state space matrices are

$$\mathbf{A} = \begin{bmatrix} 1 & T_s & 0 \\ 0 & 1 & T_s \\ 0 & 0 & 1 - T_s/\tau \end{bmatrix}$$

$$\mathbf{B} = [0 \quad 0 \quad T_s/\tau]^T$$

$$\mathbf{C} = \begin{bmatrix} 1 & 0 & 0 \\ 0 & -1 & 0 \end{bmatrix}$$

$$\mathbf{D} = 0$$

where T_s is the sampling time of the plant, and τ is the time constant (time lag) of the low-level controller.

3.2.Feasible Initial Conditions

When the host vehicle encounters a vehicle ahead, the range, range rate, and acceleration values are referred to as the initial condition of TM. A feasible initial condition scenario is when the host vehicle can decrease its velocity to reach the target vehicle velocity in time without colliding with it during TM. To find the feasible initial conditions, the system equations (Eq. (20)) should be solved to find the minimum distance required by the vehicle to stop for any given initial condition. The solution for the state equations (Eq. (20)) [5] is

$$\boldsymbol{x(t)} = \boldsymbol{e^{At}x(0)} + \int_0^t \boldsymbol{e^{A(t-\eta)}Bu(\eta)d\eta} \quad \textbf{(21)}$$

Assuming the host vehicle is moving with constant initial velocity ($v_h(0)$), and the target vehicle is also moving with constant velocity v_o; the initial conditions can be written as

$$\boldsymbol{x(0)} = \begin{bmatrix} \mathbf{0} \\ \boldsymbol{v_h(0) - v_o} \\ \mathbf{0} \end{bmatrix}$$

Given e^{At} and $x(0)$ for the maximum deceleration maneuver, the solution of a system of equations can be written as:

$$\begin{aligned} \boldsymbol{x_1(t)} &= \boldsymbol{(v_h(0) - v_o)t} \\ &\quad + \boldsymbol{(0.25 - 0.5t} \\ &\quad + \boldsymbol{0.5t^2} \\ &\quad - \boldsymbol{0.25e^{-2t})u_{min}} \\ \boldsymbol{x_2(t)} &= \boldsymbol{v_h(0) - v_o} \\ &\quad + \boldsymbol{(-0.5 + t} \\ &\quad + \boldsymbol{0.5e^{-2t})u_{min}} \\ \boldsymbol{x_3(t)} &= \boldsymbol{(1 - e^{-2t})u_{min}} \end{aligned} \quad \textbf{(22)}$$

The initial condition is said to be feasible if the initial range is greater than the d_{des} obtained, i.e., at which the range rate becomes zero.

3.3.MPC Formulation

Let the sampling instant be k_i, $k_i > 0$, the state variable vector $x(k_i)$ is available, and the length of the optimization window is N_p (also called prediction horizon), then the future control trajectory is:

$$\boldsymbol{\Delta u(k_i), \Delta u(k_i + 1), \ldots, \Delta u(k_i + N_c - 1)}$$

where N_c is called the control horizon. The future state vector is:

$$\boldsymbol{x(k_i + 1|k_i), x(k_i + 2|k_i), \ldots, x(k_i + m|k_i), \ldots, x(k_i + N_p|k_i)}$$

where $N_c \leq N_p$

Based on the state-space model, the future state variables can be evaluated:

$$x(k_i+1|k_i) = Ax(k_i) + B\Delta u(k_i)$$

$$\begin{aligned} x(k_i+2|k_i) &= Ax(k_i+1) \\ &\quad + B\Delta u(k_i+1) \\ &= A^2\, x(k_i) \\ &\quad + AB\Delta u(k_i) \\ &\quad + B\Delta u(k_i+1) \end{aligned}$$

$$\vdots$$

$$\begin{aligned} x(k_i+N_p|k_i) &= A^{N_p}\, x(k_i) \\ &\quad + A^{N_p-1}B\Delta u(k_i) \\ &\quad + A^{N_p-2}B\Delta u(k_i+1) \\ &\quad + \cdots \\ &\quad + A^{N_p-N_c}B\Delta u(k_i \\ &\quad + N_c - 1) \end{aligned} \qquad (23)$$

By substitution, the output can be calculated as:

$$y(k_i+1|k_i) = CAx(k_i) + CB\Delta u(k_i)$$

$$\begin{aligned} y(k_i+2|k_i) &= CA^2\, x(k_i) \\ &\quad + CAB\Delta u(k_i) \\ &\quad + CB\Delta u(k_i+1) \end{aligned} \qquad (24)$$

$$\vdots$$

$$\begin{aligned} y(k_i+N_p|k_i) &= CA^{N_p}\, x(k_i) \\ &\quad + CA^{N_p-1}B\Delta u(k_i) \\ &\quad + CA^{N_p-2}B\Delta u(k_i \\ &\quad + 1) + \cdots \\ &\quad + CA^{N_p-N_c}B\Delta u(k_i \\ &\quad + N_c - 1) \end{aligned}$$

Rewrite the equations in a vector form:

$$\begin{aligned} Y = [\,&y(k_i+1|k_i) \quad y(k_i+2|k_i) \quad y(k_i \\ &+ 3|k_i) \ldots y(k_i+N_p|k_i)\,]^T \end{aligned}$$

$$\begin{aligned} \Delta U = [\,&\Delta u(k_i) \quad \Delta u(k_i+1) \quad \Delta u(k_i \\ &+ 2) \ldots \Delta u(k_i+N_c-1)\,]^T \end{aligned}$$

Collecting Eqs. (23) and (24) in a compact matrix form to get:

$$Y = Gx(k_i) + \Phi\Delta U \qquad (25)$$

where

$$G = \begin{bmatrix} CA \\ CA^2 \\ CA^3 \\ \vdots \\ CA^{N_p} \end{bmatrix}$$

$$\Phi = \begin{bmatrix} CB & 0 & 0 & \ldots & 0 \\ CAB & CB & 0 & \ldots & 0 \\ CA^2B & CAB & CB & \ldots & 0 \\ \vdots & & & & \\ CA^{N_p-1}B & CA^{N_p-2}B & CA^{N_p-3}B & \ldots & CA^{N_p-N_c}B \end{bmatrix}$$

To solve the MPC problem at every iteration, a general cost function as given in [24] is defined. This cost function is defined as follows:

$$J = (R_s - Y)^T(R_s - Y) + \Delta U^T \bar{R}\Delta U \qquad (26)$$

where R_s is the data vector containing the set-point value,

$$R_s{}^T = \overbrace{[1 \quad 1 \quad \ldots \quad 1]}^{N_p} r(k_i)$$

where $r(k_i)$ is the given set-point signal at time instant k_i.

Now, ΔU can be optioned by:

$$\Delta U = (\Phi^T\Phi + \bar{R})^{-1}\Phi^T(R_s - Gx(k_i)) \qquad (27)$$

When ΔU vector is obtained, only the first element is applied to the present system. This vector value must be limited to an upper and lower bound according to the physical limitations of the vehicle acceleration/ deceleration values.

4.MPC FOR ADAPTIVE CRUISE CONTROL SYSTEM

4.1.Formulation of MPC as an Optimal Control Problem

An online optimal control problem (OCP) is solved using a receding-horizon approach to obtain state feedback control variables. State space representation of the two vehicles model (Fig.9) can be formed by rewriting Eq. (20) as

$$X(k+1) = \mathbf{A}\, X(k) + \mathbf{B}\, \mathbf{u}(k)$$

$$y = \Upsilon X(k) \qquad (28)$$

where $X = [\Delta_e \quad \Delta_v \quad \ddot{x}]^T$

$\Upsilon = \begin{bmatrix} -1 & 0 & 0 \\ 0 & -1 & 0 \end{bmatrix}$

By choosing the range error Δ_e and relative velocity Δ_v as the output variables, the output vector becomes:

$$y = [\Delta_e \quad \Delta_v]$$

4.2.Cost Function and Constraints

The control objectives and other constraints necessary for the formulated control problem are as follows:

$$\begin{aligned} J_N(x_0, u) &= V_f(x(N)) \\ &\quad + \sum_{k=0}^{N-1} l(x(k), u(k)) \\ s.t. \quad & u \in \mathbb{U}, x \in \mathbb{X} \end{aligned} \qquad (29)$$

$$\begin{aligned} J_N(x_0, u) &= x(N)^T S x(N) \\ &\quad + \sum_{k=0}^{N-1} x(k)^T Q x(k) \\ &\quad + u(k)^T R u(k) \end{aligned} \qquad (30)$$

where S, Q, and R are nonnegative weighting matrices, and N is the time horizon.

Several constraints should be considered to obtain realizable calculated results of the designed controller, as follows

1- Control constraints: This physical constraint related to the ACC vehicle defines the limit of acceleration, and it is assumed to range between u_{max} ($0.25{\times}g\ m/s^2$) and u_{min} ($-0.5 \times g\ m/s^2$).

$$u_{min} \leq \Delta u(k) \leq u_{max}$$

2- State constraints: They define the limits of distance error Δ_e and range rate Δ_v, which

must satisfy the feasible initial condition mentioned in Section 3.2 to avoid collision between the two vehicles:

$\Delta_e \geq d_{des}$ (collision avoidance)

$\Delta_v \leq v_l$ (guarantees $v_h \geq 0$)

3- Terminal constraints: They refer to the final state values of the model states, which must all converge to zero:

$$\boldsymbol{x(N)} = \begin{bmatrix} \Delta_e \\ \Delta_v \\ \ddot{x} \end{bmatrix} = \begin{bmatrix} \mathbf{0} \\ \mathbf{0} \\ \mathbf{0} \end{bmatrix}$$

The whole problem of the performance index and the constraint equations forms a mathematical program (MP). The solution is then obtained using a mathematical programming solver. The control inputs are calculated by solving the OCP below during each simulation time step.

$$\boldsymbol{min_u\, J = x(N)^T S x(N) + \sum_{k=0}^{N-1} x(k)^T Q x(k) + u(k)^T R u(k)} \quad \textbf{(31)}$$

s.t

$$\boldsymbol{u_{min} \leq \Delta u(k) \leq u_{max}}$$
$$\boldsymbol{-x_1(k) \leq d_{des}}$$
$$\boldsymbol{x_2(k) \leq v_l}$$
$$\boldsymbol{x(N) = [0 \quad 0 \quad 0]^T}$$

4.3.Two-Step Prediction MPC Algorithm

Real-Time Iteration (RTI) is a method created for nonlinear optimization in optimal feedback control and used by Villarreal and Rossiter [21] to determine real-time performance based on several strategies. One of these strategies is Initial Value Embedding (IVE), which uses a shifted version of the solution determined in the prior step to obtain the nominal trajectory [21]. Recursive feasibility, in which a given solution at the current time is feasible, and then all following solutions at future times also remain feasible, is an important property to preserve in an optimization technique. Recursive feasibility is guaranteed if the optimization includes the solution from the prior time step as a possible solution of the current optimization (called the tail). An approach that decreases the computational burden for the MPC, which is based on IVE with a two-step prediction, is presented in the present paper. In this method, the tail is used as a solution in time step k, and the average of two control inputs, namely, Uk_i and Uk_{i+1}, is used as a solution in time step k+1. This method simulates a parallel calculation inside the optimization algorithm. The proposed scheme helped reduce the execution time of the algorithm at the cost of increasing the commanded acceleration fluctuation. However, this fluctuation is considered acceptable and within the permitted range.

The algorithm is illustrated below:

Algorithm 1: Implementation of the MPC algorithm

(1) Driving Mode Selection: sense the road ahead
If no preceding vehicle occurs **Then** keep CC mode **Goto (5)**
Elseif a preceding vehicle is encountered **Then** switch to ACC mode.
(2) Measure range and range rate and formulate OCP to compute the optimal input $\boldsymbol{u}$ using the proposed MPC, which represents the desired acceleration $\ddot{\boldsymbol{x}}_{\boldsymbol{des}}$.
(3) Compute the desired throttle and brake signal that tracks $\ddot{\boldsymbol{x}}_{\boldsymbol{des}}$.
(4) If the preceding vehicle stopped, **Goto (6)**
Else Goto (2)
(5) Set $\boldsymbol{v_h = v_{des}}$ Goto (1)
(6) Stop and **End.**

5.SIMULATION RESULTS

The proposed control scheme was investigated for two traffic situations based on the longitudinal dynamic model of the host vehicle to evaluate the control algorithm. The sampling time T was 0.1s. Q, R, and S matrices were chosen to be identity matrices. The controller algorithm and the host vehicle's response were performed using MATLAB. In the first scenario, the ACC vehicle traveled with a constant cruise speed of 20 m/s (CC mode), and then a halted leading vehicle was detected. The initial gap spacing between the two vehicles was set to 110 m. The control law found by the algorithm is successful if the ACC vehicle can maneuver to the desired gap distance without colliding with the preceding vehicle. In Fig. 11(a), the inter-vehicle distance can be seen starting from 110 and ending at zero, which is the intended range error. Figure 11(b) shows the velocity profile of the host and target vehicles. The target vehicle speed was zero, while the ACC vehicle decelerated from its initial speed (20 m/s) to zero as it encountered a stopped vehicle ahead.

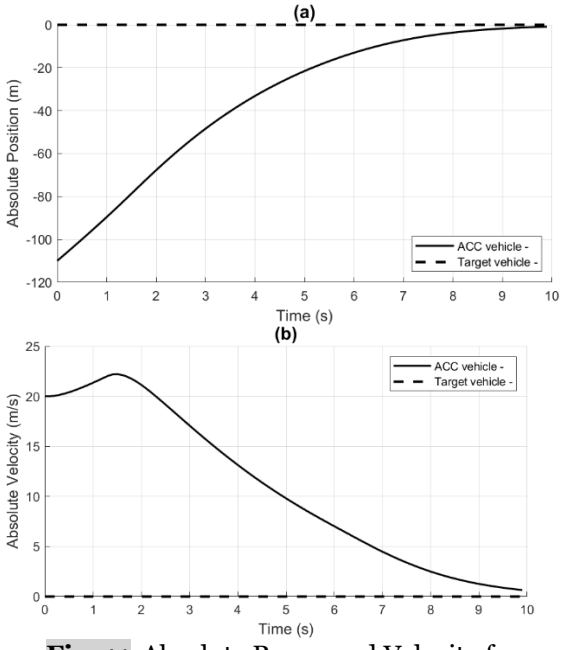

Fig. 11 Absolute Range and Velocity for Scenario 1.

In Fig.12 (a) and (b), the solid black line shows that in the case of constrained deceleration, the

host vehicle maneuvered the preceding vehicle to the desired distance and maintained this distance without collision. The red line represents the response of the ACC vehicle with deceleration limits applied by checking for saturation. In this case, the host vehicle collided with the stalled vehicle because the deceleration limits were not included as constraints in the formulated problem. An "x" mark is used to depict the collision point, and the dashed lines represent the ACC vehicle path once it has crossed the d_{des}. In Fig. 12 (c) and (d), the actual and the commanded acceleration calculated by the HLC MPC controller are plotted. The acceleration values of the MPC remained within the upper and lower permitted limits. In addition to the two cases' responses shown earlier, an extra case (unlimited) is illustrated in Figs. 13 and 14 to test and compare both controllers' performances.

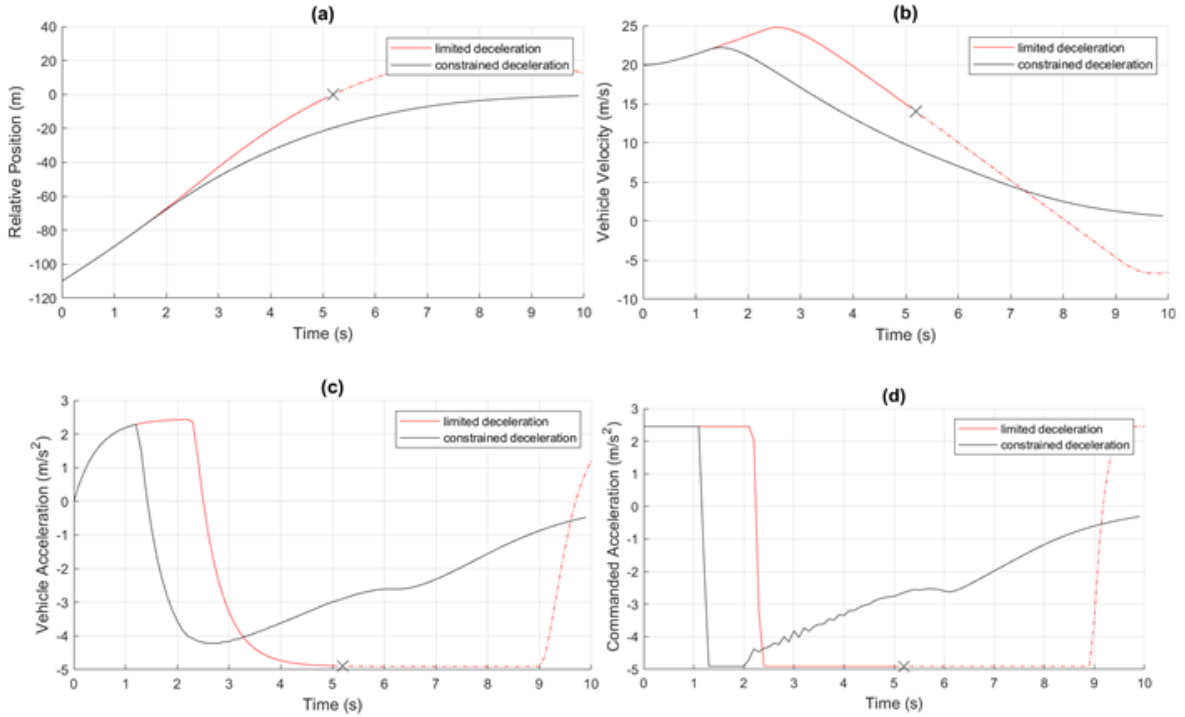

Fig. 12 Two Cases Deceleration for Scenario 1.

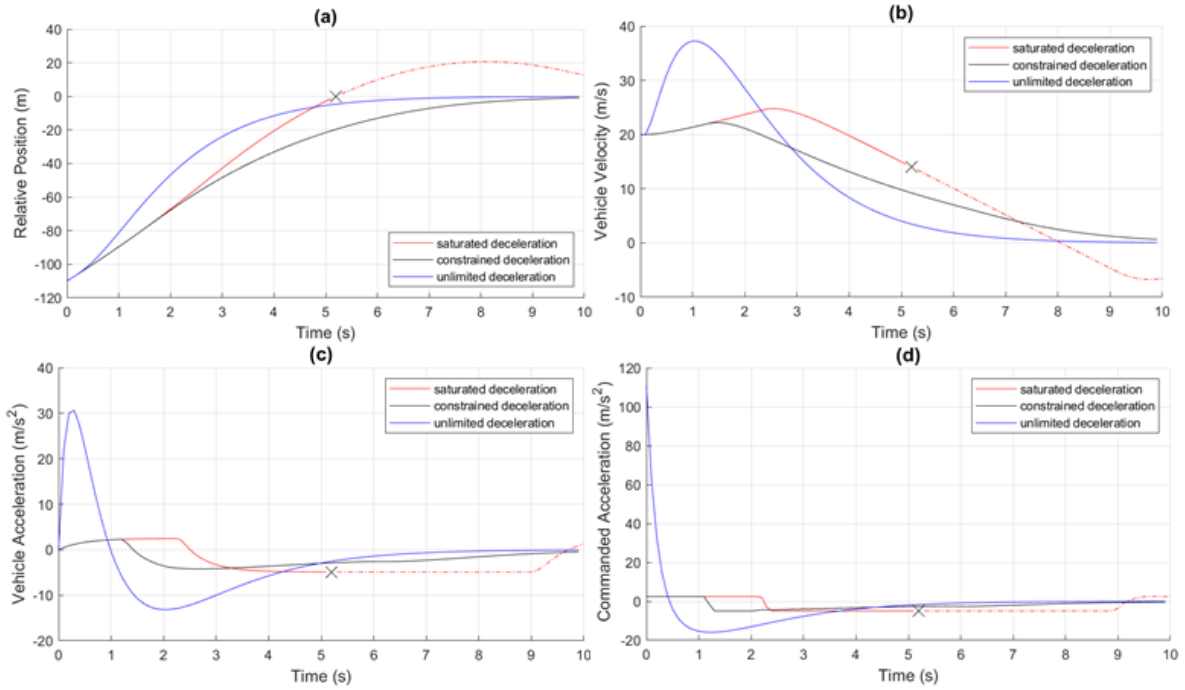

Fig. 13 Three Cases Simulations for Scenario 1 with Original MPC.

The execution time was approximately 1.1 s and 0.8 s for the original MPC and speedup MPC controllers, respectively. The fluctuation mentioned in the previous section can be seen in the three deceleration cases (Fig. 14 (c) and (d)). No collision occurred in the unlimited deceleration case, yet it can be neglected since it is not applicable practically and is plotted for analytical purposes only.

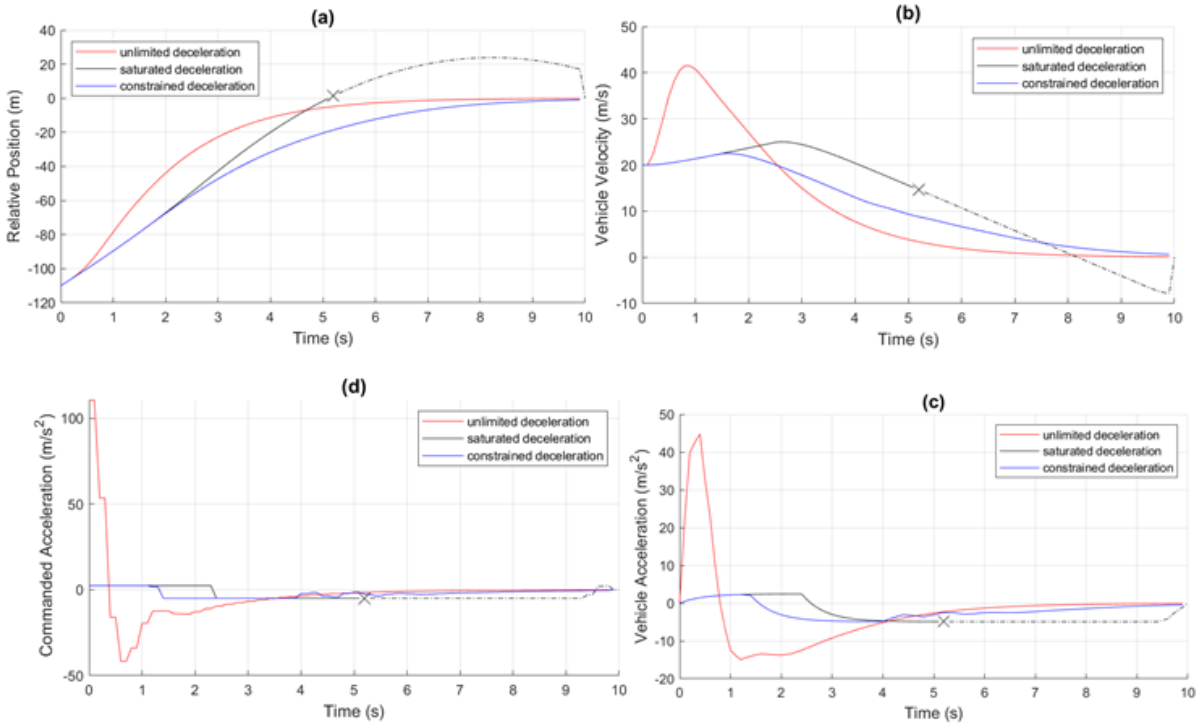

Fig. 14 Three Cases Simulations for Scenario 1 with Speedup MPC.

In the second scenario, the ACC vehicle encountered an accelerating leading vehicle. The simulation was initialized with 30 m/s (CC mode) for the ACC vehicle and an accelerating preceding vehicle at a range rate of 20 m/s. First, the initial distance between the two vehicles was 60 m. Then, the preceding vehicle accelerated and maintained a speed of 27 m/s. Figure 15 shows the ACC vehicle's response to the control command with the original MPC. It shows that the control input initially commanded the host vehicle to decelerate as the target was encountered. Since the gap between the two vehicles increased due to the accelerating target vehicle, a control command instructed the host vehicle to accelerate. The ACC vehicle maneuvered the target vehicle successfully without collision. It can be noticed from Fig. 16 that the ACC vehicle acted similarly and maintained the desired spacing ahead. The simulation shows that the ACC vehicle first decreased its velocity to track the target vehicle, and then it settled down, approximately after five seconds, to the steady-state value.

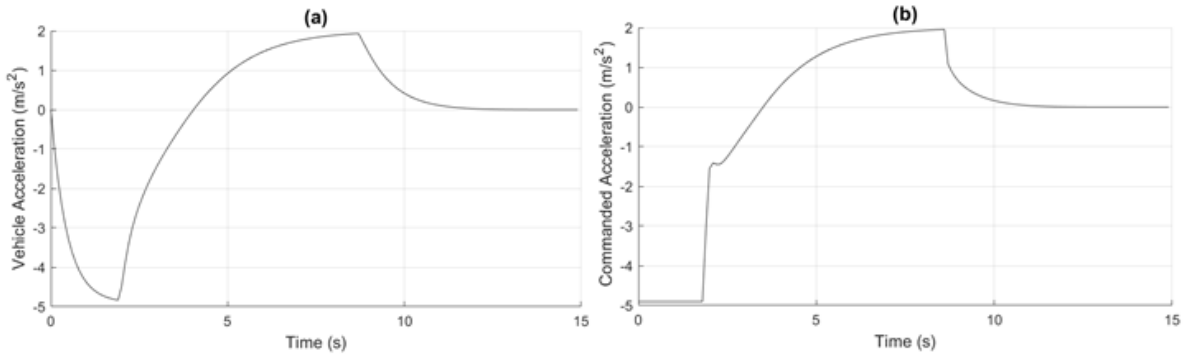

Fig. 15 Host Vehicle Response for Scenario 2 with Original MPC.

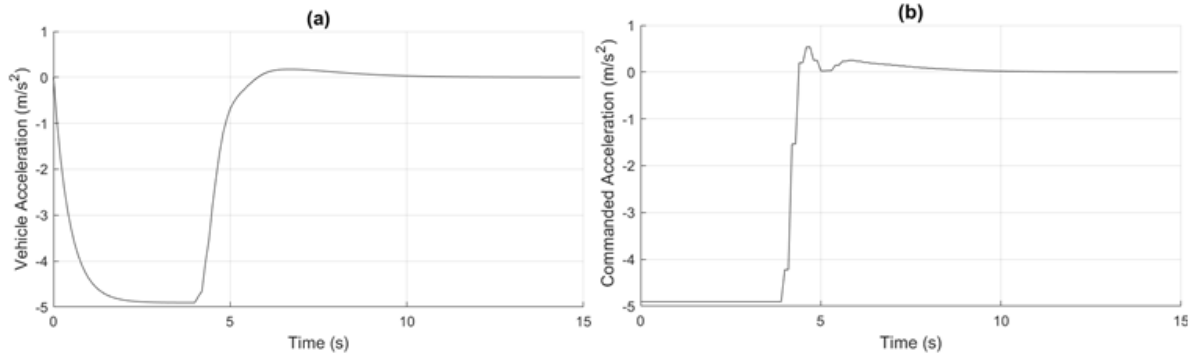

Fig. 16 Host Vehicle Response for Scenario 2 with Speedup MPC.

From Fig. 17 (a) and (b), it can be seen that input control initially decreased the host vehicle speed as the target was encountered. Still, since the target vehicle continuously accelerated, the controller commanded the ACC vehicle to increase its speed after 5 seconds of simulation to track the target vehicle ahead. Both controllers performed similarly; however, the proposed algorithm outperformed the original controller in terms of execution time. The algorithm for the original MPC took 0.226 s, while the speedup MPC took 0.130 s. To simulate real-world disturbances and uncertainties due to noise or inaccurate measurement by the sensor, a third scenario was tested. This scenario is similar to the second one but with a randomized speed trace for the target vehicle to emulate variability in driving, as shown in Fig. 18 (b) and Fig. 19 (b).

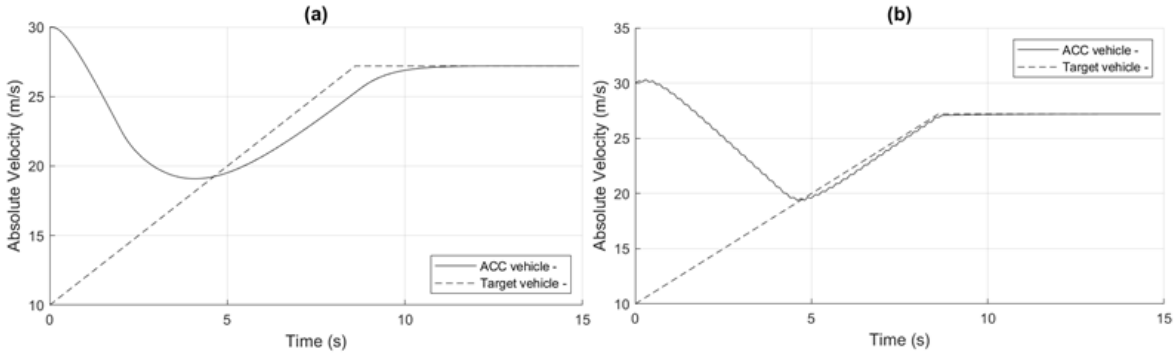

Fig. 17 Host Vehicle Response of Both Controllers for Scenario 2 (a) Original MPC, (b) Speed up MPC.

It can be seen that the proposed method outperformed the simple MPC for both the vehicle's acceleration and commanded acceleration. The error in the target vehicle speed affected the calculated acceleration for the ACC vehicle in the original MPC controller (Fig. 18 (c) and (d)). In contrast, in the proposed method, the error was canceled (Fig. 19 (c) and (d)). This behavior happened due to the inherent recursive feasibility property of the proposed strategy that uses two tails of control inputs (past and current) as possible solutions for the next step.

6.CONCLUSIONS

The following conclusions can be drawn from the present study results:

- A High-level controller for the ACC system based on MPC was designed and simulated.
- A method to increase the efficiency of computations was presented.
- Two driving scenarios were used to evaluate and compare the effectiveness of the proposed algorithm, showing a successful transitional maneuver and collision avoidance for the ACC vehicle.
- A collision occurred when starting with an infeasible scenario. As an example of infeasible initial conditions, the initial range between the two vehicles was less than the required distance to perform a full-stop brake. In addition, when a deceleration limit was not involved as a constraint in formulating the control problem, it led to nonrealistic control input.
- The proposed controller performance was better in terms of computation efforts and measurement uncertainty. Moreover, reducing computational effort and stability are conflicting objectives, so a balance based on the design requirements is required for an acceptable result. This conflict was apparent when a reduction in computational time led to fluctuations and variations in the commanded control input of the controller.

ACKNOWLEDGEMENTS

The authors are grateful for the financial support toward this research by the Electrical Engineering Department, College of Engineering, University of Baghdad. Postgraduate Research Grant (PGRG) No. (18s/211) in (10/01/2023.)

NOMENCLATURE

A	Frontal area of the vehicle, m^2
C_r	Rolling resistance coefficient
C_d	Aerodynamic resistance coefficient
C_{sr}	Speed ratio
C_{tr}	Torque ratio
F_{xf}	Front longitudinal tire force, N
F_{xr}	Rear longitudinal tire force, N
F_{aero}	Longitudinal aerodynamic drag force, N
F_z	Normal force exerted on the tire, N
g	Gravitational constant, m/s^2
J_w	Moment of inertia of the wheels Kg. m^2
K_{tc}	Capacity factor
m	Mass of the vehicle, Kg
R_{xf}	Rolling resistance force at the front tires, N
R_{xr}	Rolling resistance force at the rear tires, N
R_w	Wheel radius, m
R_{tr}	Transmission ratio
T_t	Output torque of the converter, N. m
T_i	Input torque of the converter, N. m
T_{out}	Transmission output torque, N. m
T_{in}	Transmission input torque, N. m
T_w	Wheel torque, N. m
T_b	Brake torque, N. m
V	Vehicle's speed, m/s
$\ddot{x}$	Acceleration of the vehicle, m/s^2
Greek symbols	
η_c	Efficiency factor
θ	Road's angle of inclination, rad
ρ	Mass density of the air, kg/m^3
$\dot{\omega}$	Angular acceleration of the wheel, rad/s
ω_t	Output speed, rad/s
ω_i	Output speed, rad/s
ω_e	Engine rotation speed, rad/s

REFERENCES

[1] Sun C, Chu L, Guo J, Shi D, Li T, Jiang Y. **Research on Adaptive Cruise Control Strategy of Pure Electric Vehicle with Braking Energy Recovery**. *Advances in Mechanical Engineering* 2017; **9**(11): 1–12.

[2] Shaleesh IS, Almohammedi AA, Mohammad NI, Ahmad AA, Shepelev V. **Cooperation and Radio Silence Strategy in Mix Zone to Protect Location Privacy of Vehicle in VANET**. *Tikrit Journal of Engineering Sciences* 2021; **28**(1): 31–39.

[3] Gustavsson P, Aust ML. **In-Vehicle Nudging for Increased Adaptive Cruise Control Use: A Field Study**. *Journal on Multimodal User Interfaces* 2024; **18**(1): 1–12.

[4] Mohammed D, Nagy V, Márton L, Jagicza M, Józsa D, Horváth B. **Efficiency of Adaptive Cruise Control in Commercial Vehicles**. *Pollack Periodica* 2024; **19**(1): 1–7.

[5] Bageshwar VL, Garrard WL, Rajamani R. **Model Predictive Control of Transitional Maneuvers for Adaptive Cruise Control Vehicles**. *IEEE Transactions on Vehicular Technology* 2004; **53**(5): 1573–1585.

[6] Shakouri P, Ordys A, Laila DS, Askari MR. **Adaptive Cruise Control System: Comparing Gain-Scheduling PI and LQ Controllers**. In: *Proceedings of the 18th IFAC World Congress*. Milano, Italy; 2011. pp. 12956–12961.

[7] Zhu Z, Bei S, Li B, Liu G, Tang H, Zhu Y, Gao C. **Research on Robust Control of Intelligent Vehicle Adaptive Cruise**. *World Electric Vehicle Journal* 2023; **14**(5): 127.

[8] Ahmed DF, Abed IA. **Model Predictive Control of a Double Effect Evaporator Via Simulation**. *Tikrit Journal of Engineering Sciences* 2021; **28**(1): 49–63.

[9] Alkareem MS, Abbas NH. **Model Predictive Control Design for Electric Vehicle Based on Improved Physics-Inspired Optimization Algorithms**. *Tikrit Journal of Engineering Sciences* 2023; **30**(4): 118–126.

[10] Ali LM, Al-Zughaibi AI. **Investigation of Control Behavior via Active Suspension System Considering Time-Delay and Variable Masses**. *Journal of Engineering* 2024; **30**(11): 108–127.

[11] Mahadika P, Subiantoro A, Kusumoputro B. **Neural Network Predictive Control Approach Design for Adaptive Cruise Control**. *International Journal of Technology* 2020; **11**(7): 1451–1462.

[12] Jai Y, Jibrin R, Itoh Y, Gorges D. **Energy-Optimal Adaptive Cruise Control for Electric Vehicles in Both Space Domain based on Model Predictive Control**. *IFAC-PapersOnLine* 2019; **52**(5): 316–321.

[13] Feng S, Zhao Y, Deng H, Wang Q. **Binary Search Tree-Based Explicit MPC Controller Design with Kalman Filter for Vehicular Adaptive Cruise System**. *Proceedings of the Institution of Mechanical Engineers, Part D: Journal of Automobile Engineering* 2021; **235**(13): 3183–3196.

[14] Yang Z, Wang Z, Yan M. **An Optimization Design of Adaptive Cruise Control System Based on MPC and ADRC**. *Actuators* 2021; **10**(7): 144.

[15] Zhan Y, Zhai C, Long X, Wang B, Chen H, Chen C. **Robust Optimal Adaptive Cruise Control Based on ADP for Intelligent Vehicles under Bounded Disturbances**. In: *2023 7th CAA International Conference on Vehicular*

Control and Intelligence (CVCI). IEEE; 2023. pp. 1–6.

[16] Mahdinia I, Arvin R, Khattak AJ, Ghiasi A. **Safety, Energy, and Emissions Impacts of Adaptive Cruise Control and Cooperative Adaptive Cruise Control**. *Transportation Research Record: Journal of the Transportation Research Board* 2020; **2674**(4): 253–267.

[17] Shakouri P, Ordys A. **Nonlinear Model Predictive Control Approach in Design of Adaptive Cruise Control with Automated Switching to Cruise Control**. *Control Engineering Practice* 2014; **26**: 160–177.

[18] Guo L, Ge P, Sun D, Qiao Y. **Adaptive Cruise Control Based on Model Predictive Control with Constraints Softening**. *Applied Sciences* 2020; **10**(6): 2117.

[19] Nie Z, Farzaneh H. **Adaptive Cruise Control for Eco-Driving Based on Model Predictive Control Algorithm**. *Applied Sciences* 2020; **10**(15): 5271.

[20] Capuano A, Spano M, Musa A, Toscano G, Misul D. **Development of an Adaptive Model Predictive Control for Platooning Safety in Battery Electric Vehicles**. *Energies* 2021; **14**(13): 3912.

[21] Villarreal O, Rossiter JA. **A Shifting Strategy for Efficient Block-based Nonlinear Model Predictive Control Using Real-Time Iterations**. *IET Control Theory & Applications* 2020; **14**(19): 3275–3284.

[22] Cho D, Hedrick JK. **Automotive Powertrain Modeling for Control**. *Journal of Dynamic Systems, Measurement, and Control* 1989; **111**(4): 568–576.

[23] Rajamani R. **Vehicle Dynamics and Control**. 2nd ed. Springer: New York, USA; 2012.

[24] Wong JY. **Theory of Ground Vehicles**. 4th ed. John Wiley & Sons: Hoboken, NJ, USA; 2008.

[25] Pacejka HB. **Tire and Vehicle Dynamics**. 3rd ed. Butterworth-Heinemann: Oxford, UK; 2012.

[26] Memon Z, Unar MA, Pathan DK. **Parametric Study of Nonlinear Adaptive Cruise Control for a Road Vehicle Model by MPC**. *Mehran University Research Journal of Engineering & Technology* 2012; **31**(2): 301–314.

[27] Wang L. **Model Predictive Control System Design and Implementation Using MATLAB®**. Springer: London, UK; 2009.